AFM Imaging of Ligand Binding to Platelet Integrin α IIb β 3 Receptors Reconstituted into Planar Lipid Bilayers

ARTICLE *in* LANGMUIR · AUGUST 2005

Impact Factor: 4.46 · DOI: 10.1021/la046943h · Source: PubMed

3 AUTHORS, INCLUDING:

Mohammad Hussain
King Abdulaziz University
37 PUBLICATIONS **519** CITATIONS

SEE PROFILE

AFM Imaging of Ligand Binding to Platelet Integrin $\alpha_{IIb}\beta_3$ Receptors Reconstituted into Planar Lipid Bilayers

Mohammad A. Hussain,[†] Aashiish Agnihotri,[‡] and Christopher A. Siedlecki*[,†,‡]

Departments of Surgery and Bioengineering, The Biomedical Engineering Institute, The Milton S. Hershey Medical Center, The Pennsylvania State University, Hershey, Pennsylvania 17033

Received December 13, 2004. In Final Form: May 13, 2005

The platelet integrin $\alpha_{IIb}\beta_3$ plays a key role in platelet adhesion, activation, and aggregation at the subendothelium and at protein-coated synthetic biomaterials. In this study, interactions between $\alpha_{IIb}\beta_3$ and both protein and peptide ligands for the receptor were imaged under physiological conditions by high-resolution atomic force microscopy (AFM). To directly image the ligand−receptor interactions, $\alpha_{IIb}\beta_3$ receptors were reconstituted into a supported lipid bilayer formed on a mica surface in the AFM fluid cell assembly and subsequently activated with Mn^{2+}. Fibrinogen, the natural protein ligand for the integrin, as well as a nanogold-labeled peptide ligand (an RGD-containing heptamer) were infused into the AFM fluid cell, incubated with the reconstituted and activated receptors, and imaged under buffer. Height images illustrating topographical features showed the integrin reconstituted in the bilayer. Fibrinogen molecules binding to the receptors were easily observed in the height images, with fibrinogen showing its characteristic trinodular structure and occasionally bridging integrin receptors. Fibrinogen was observed to bind to integrins at the D-domain consistent with the location of the γ-chain dodecapeptide, while fibrinogen bridging integrins bound to receptors on opposite sides of the protein consistent with a 2-fold axis of symmetry. Peptide ligands were not visible in height images; however, phase images that map the mechanical properties detected the nanogold labels and demonstrated the presence of peptide ligands bound to the receptors. The results demonstrate the ability of this high-resolution microscopy technique to directly visualize single ligand/receptor interactions in a dynamic and physiologically relevant environment, and establish a framework for future fundamental studies of single protein/receptor interactions during normal pathological processes as well as biomaterial surface-induced thrombosis.

Introduction

The platelet integrin $\alpha_{IIb}\beta_3$ is a calcium-dependent heterodimer present in very high numbers on platelet membranes, and is responsible for mediating platelet−subendothelium, platelet−biomaterial, and platelet−platelet interactions.[1,2] Electron microscopy studies show the integrin to consist of an 8 × 12 nm head with two 18 nm flexible tails,[3] while atomic force microscopy (AFM) reveals slightly larger hydrated globular head dimensions, 14.9 nm across × 14.4 nm long × 3.1 nm tall, with an 18.6 nm long tail, due in part to lateral expansion of the dimensions by the atomic force microscopy probe tip.[4] This integrin plays a central role in platelet aggregation during hemostasis, thrombosis, and wound healing[5,6] by binding to soluble proteins present in plasma such as fibrinogen, von Willebrand factor, and fibronectin, as well as to the subendothelium. Defects in platelet integrins lead to bleeding disorders, as demonstrated in patients with Glanzmann's thrombasthenia.[7−9]

Fibrinogen is an important ligand for $\alpha_{IIb}\beta_3$, as it is the third most abundant soluble protein in blood and has multiple binding sites for the integrin. Furthermore, fibrinogen/$\alpha_{IIb}\beta_3$ interactions are known to be important in the development of biomaterial-induced thrombosis, a significant impediment to the development of medical devices intended for use in blood-contacting applications.[10] The γ-chain dodecapeptide, located in the C-terminal region of the fibrinogen γ-chain (residues 400−411), has been shown to be critical for platelet adhesion.[11,12] Another important integrin ligand is the ubiquitous tripeptide sequence Arg-Gly-Asp (RGD), a common amino acid motif found in a number of adhesive proteins.[13] These ligands inhibit the adhesion of platelets to protein-coated surfaces as well as inhibit platelet/platelet aggregation by binding to the platelet integrin receptor $\alpha_{IIb}\beta_3$.

Biologists have traditionally relied on ensemble properties obtained through biochemical techniques such as measurement of binding affinities or reaction rate constants to study ligand−receptor interactions. In the past few decades, a new trend focusing on individual biomolecular measurements has been seen, due in large part to advancements in optical and mechanical methods for measuring interactions. The interactions of individual biomolecule events have been explored using powerful techniques including fluorescence resonant energy transfer (FRET), total internal reflection fluorescence (TIRF)[14−16] and optical tweezers.[17−19]

* To whom correspondence should be addressed. Phone: (717) 531-5716. Fax: (717) 531-4464. E-mail: csiedlecki@psu.edu.
[†] Department of Surgery.
[‡] Department of Bioengineering.

(1) Ginsberg, M. H.; Du, X.; O'Toole, T. E.; Loftus, J. C. *Thromb. Haemostasis* **1995**, *74*, 352.
(2) Calvete, J. J. *Thromb. Haemostasis* **1994**, *72*, 1.
(3) Weisel, J. W.; Nagaswami, C.; Vilaire, G.; Bennett, J. S. *J. Biol. Chem.* **1992**, *267*, 16637.
(4) Hussain, M. A.; Siedlecki, C. A. *Micron* **2004**, *35*, 565.
(5) Marguerie, G. A.; Edgington, T. S.; Plow, E. F. *J. Biol. Chem.* **1980**, *255*, 154.
(6) Kieffer, N.; Phillips, D. R. *Annu. Rev. Cell Biol.* **1990**, *6*, 329.
(7) Tullu, M. S.; Dixit, P. S.; Nair, S. B.; Kamat, J. R.; Vaswani, R. K.; Shetty, S. D.; Pawar, A. R. *Indian J. Pediatr.* **2001**, *68*, 563.
(8) Tomiyama, Y. *Int. J. Hematol.* **2000**, *72*, 448.
(9) Boudreaux, M. K.; Lipscomb, D. L. *Vet. Pathol.* **2001**, *38*, 249.
(10) Horbett, T. A. *Cardiovasc. Pathol.* **1993**, *2*, 137S.
(11) Farrell, D. H.; Thiagarajan, P. *J. Biol. Chem.* **1994**, *269*, 226.
(12) Farrell, D. H.; Thiagarajan, P.; Chung, D. W.; Davie, E. W. *Proc. Natl. Acad. Sci. U.S.A.* **1992**, *89*, 10729.
(13) D'Souza, S. E.; Ginsberg, M. H.; Plow, E. F. *Trends Biochem. Sci.* **1991**, *16*, 246.

10.1021/la046943h CCC: $30.25
Published on Web 06/23/2005

The atomic force microscope[20] has proven to be another important tool for the study of single proteins in physiologically relevant environments. Because the atomic force microscope does not require a vacuum environment for imaging, it offers the opportunity to look at the structure of single molecules under aqueous buffer, an advantage over "dry" techniques such as X-ray crystallography and electron microscopy. AFM studies looking at protein function and protein interactions have largely, though not exclusively, focused on measuring the strength of receptor−ligand interactions, including studies measuring the unbinding force involved between the $\alpha_{IIb}\beta_3$ receptor and its ligands.[21,22] More recently, integrin $\alpha_5\beta_1$ was immobilized on AFM probes, and the interaction with RGD and the synergy binding site was measured down to the single-molecule level.[23]

Gold bead labels for measuring ligand binding to platelets have been used extensively, particularly by Albrecht and colleagues.[24−26] In these studies, fibrinogen or antibodies to the $\alpha_{IIb}\beta_3$ integrin are conjugated to gold beads and visualized by dynamic high-resolution video-enhanced light microscopy as the ligands bind to the platelets, so that motion of the integrin can be monitored by following the position of the bead. Alternatively, the gold bead labels can be used in high-resolution scanning electron microscopy (HRSEM) imaging after the platelets are fixed. Eppell et al. used similar gold bead techniques to perform a correlated AFM/HRSEM study of single platelets that had been fixed and dried.[27]

In the work described in this paper, interactions between $\alpha_{IIb}\beta_3$ receptors and the protein ligand fibrinogen as well as an RGD peptide ligand were imaged under physiological buffer conditions. As peptide ligands are too small to be detected via AFM topography images, the peptides were labeled with small (1.4 nm diameter) gold nanoparticles. These data demonstrate the ability of the atomic force microscope to image single-molecule binding by directly visualizing interactions between both RGD peptide ligands and fibrinogen ligands and $\alpha_{IIb}\beta_3$ molecules reconstituted into planar lipid bilayers.

Materials and Methods

General Procedures. All water was from a Millipore Simplicity 185 system utilizing dual UV filters (185 and 254 nm) to reduce carbon contamination. Glassware was cleaned thoroughly with Liquinox detergent and rinsed sequentially with tap water, ethanol, and Millipore water. The AFM fluid cell and other accessories including polypropylene connectors, silicone O rings, and silicone tubing were cleaned with 1% (w/v) solutions of sodium dodecyl sulfate (SDS; Sigma Chemicals, St. Louis, MO) followed by final rinses with Millipore water and drying with N_2 before use. Additional cleaning of the glass fluid cell was done by washing in a 1 N HCl bath overnight as needed. Purified human integrin $\alpha_{IIb}\beta_3$ was purchased from Enzyme Research Labs (South Bend, IN) as a 2.15 mg/mL solution in Tris buffer (pH 7.5) and stabilized with 50% (v/v) glycerol and 0.1% (v/v) Triton X-100 detergent. Fibrinogen was from Calbiochem (La Jolla, CA) and was received from the manufacturer as >95% clottable. An RGD-containing peptide (GRGDSPK) was purchased from Sigma Chemicals (St. Louis, MO) and used without further purification.

Atomic Force Microscopy. All images were collected with a MultiMode atomic force microscope with a Nanoscope IIIa controller (Digital Instruments Inc., Santa Barbara, CA). An E scanner (max scan size ~14 μm × 14 μm × 4 μm) and high aspect ratio carbon tips (EBD-Tips, Nanotools, Germany) on triangular Si_3N_4 cantilevers (spring constant ~0.6 N/m) were used to obtain images of the samples. All images were first-order flattened prior to analysis to remove sample tilt. All images were collected using the fluid tapping mode, which measures topography by intermittently contacting the surface with the tip, thereby reducing lateral forces that can damage soft samples. The tip oscillation frequency in these experiments was approximately 10 kHz. Gold beads were located using the phase signal, which generates contrast by differences in the mechanical properties across the sample.

Nanogold Labeling of Peptides. Sulfo-*N*-hydroxysuccinimido nanogold (MW 15000), a 1.4 nm diameter gold particle, was obtained from Nanoprobes, Inc. (Yaphank, NY). Nanogold coupling of RGD-containing peptide was performed according to the procedure supplied by the manufacturer. Briefly, the peptides were reacted with the nanogold reagent for 1 h at room temperature in HEPES buffer (pH 7.5). Peptides were 20−40-fold in excess of the nanogold molar concentration to ensure that most nanogold in the reaction mixture was conjugated. Unconjugated peptides were separated from nanogold-coupled peptides using gel exclusion chromatography with a prepacked PD-10 column with Sephadex G25 M having a size exclusion limit of 5 kDa (Amersham Biosciences, Piscataway, NJ). A sodium phosphate (0.02 M) buffer with 150 mM sodium chloride at pH 7.4 was used to elute the concentrated reaction mixture. The conjugate was collected as the first peak, colored a pale yellow-brown, while the subsequent colorless collection samples were discarded.

Imaging Ligand−Receptor Complexes in the Absence of Detergent. Nanogold-conjugated RGD-containing peptide and fibrinogen ligands were incubated with $\alpha_{IIb}\beta_3$ in the presence of 2 mM Mn^{2+} (to activate the integrin) at room temperature for 1−2 h. The molar ratio of ligands and $\alpha_{IIb}\beta_3$ for solution incubation was kept at 5:1 in a volume of 50 μL of Tris buffer. This reaction mixture was diluted to yield solutions of 300−500 ng/mL $\alpha_{IIb}\beta_3$ in Triton-free Tris buffer. These receptor−ligand complexes were imaged in the fluid cell by directly adsorbing to a hydrophobic highly ordered pyrolytic graphite (HOPG) substrate for 60 min, followed by an exchange for fresh protein-free buffer.

Lipid Vesicle Preparation from Egg PC. To observe single ligand−receptor binding events, the integrin was reconstituted into a supported lipid bilayer formed on a muscovite mica substrate. Egg PC (Avanti Polar Lipids, Inc., Alabaster, AL) was dissolved in 10 mM HEPES buffer, pH 7.5, with 2 mM EDTA (VWR, West Chester, PA) at a concentration of 1 mg/mL, followed by a hydration period of 2 h at room temperature. The hydrated sample was then sonicated and ultracentrifuged to obtain small unilamelar vesicles (SUVs). The SUVs were kept at 4 °C until use.

Reconstitution of Integrin into the Planar Bilayer. Reconstitution of platelet integrin molecules into the lipid bilayer was performed by first imaging a freshly cleaved mica surface in the AFM fluid cell, utilizing tapping mode AFM imaging in HEPES−EDTA buffer to ensure that the surface was appropriate for subsequent imaging. Platelet integrin was diluted to a 200−500 ng/mL final protein concentration in Tris buffer with 0.05% Triton. This protein solution was infused into the fluid cell and incubated for 30−45 min to allow adsorption of protein on the mica surface. Excess proteins, Triton, and glycerol were washed

(14) Thompson, N. L.; Lagerholm, B. C. *Curr. Opin. Biotechnol.* **1997**, *8*, 58.
(15) Muller, B.; Zerwes, H. G.; Tangemann, K.; Peter, J.; Engel, J. *J. Biol. Chem.* **1993**, *268*, 6800.
(16) Dietrich, A.; Buschmann, V.; Muller, C.; Sauer, M. *J. Biotechnol.* **2002**, *82*, 211.
(17) Arya, M.; Lopez, J. A.; Romo, G. M.; Dong, J. F.; McIntire, L. V.; Moake, J. L.; Anvari, B. *Lasers Surg. Med.* **2002**, *30*, 306.
(18) Bockelmann, U.; Thomen, P.; Essevaz-Roulet, B.; Viasnoff, V.; Heslot, F. *Biophys. J.* **2002**, *82*, 1537.
(19) Brouhard, G. J.; Schek, H. T. r.; Hunt, A. J. *IEEE Trans. Biomed. Eng.* **2003**, *50*, 121.
(20) Binnig, G.; Quate, C. F.; Gerber, C. *Phys. Rev. Lett.* **1986**, *56*, 930.
(21) Lee, I.; Marchant, R. E. *Ultramicroscopy* **2003**, *97*, 341.
(22) Lee, I.; Marchant, R. E. *Surf. Sci.* **2001**, *491*, 433.
(23) Kokkoli, E.; Ochsenhirt, S. E.; Tirrell, M. *Langmuir* **2004**, *20*, 2397.
(24) Simmons, S. R.; Albrecht, R. M. *J. Lab. Clin. Med.* **1996**, *128*, 39.
(25) Albrecht, R. M.; Goodman, S. L.; Simmons, S. R. *Am. J. Anat.* **1989**, *185*, 149.
(26) Albrecht, R. M.; Olorundare, O. E.; Simmons, S. R.; Loftus, J. C.; Mosher, D. F. *Methods Enzymol.* **1992**, *215*, 456.
(27) Eppell, S. J.; Simmons, S. R.; Albrecht, R. M.; Marchant, R. E. *Biophys. J.* **1995**, *68*, 671.

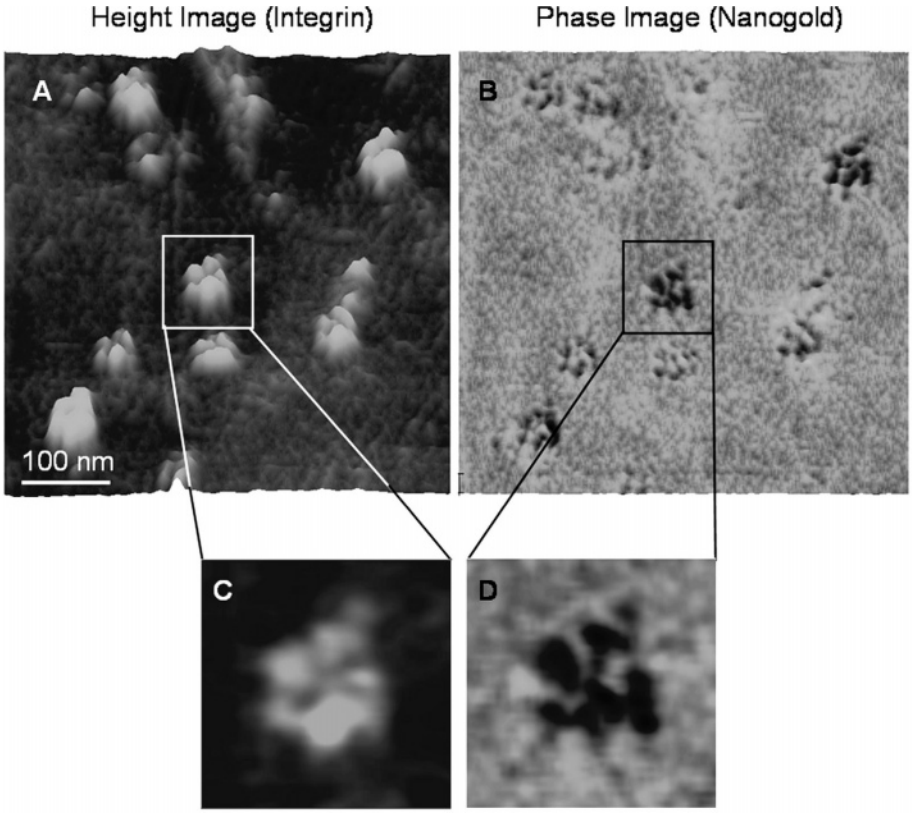

Figure 1. AFM images of RGD heptamer peptide ligand/integrin complexes imaged in detergent-free buffer after adsorption to an HOPG substrate. (A) Topographic image showing integrin aggregates arranged as rosettes. No peptides are visible in the image. (B) The phase image detects the mechanical property differences across the imaging area. Note the small black dots arising from the 1.4 nm gold-bead-labeled peptides closely associated with the aggregates. (C) Higher magnification topography image showing the individual integrins in the aggregate. There are seven receptors in this particular aggregate. (D) Phase image of the same area showing a dark spot associated with each integrin, indicating binding of the gold-labeled RGD peptide ligand. The *Z* scale is 3 nm for all topography images. (A) and (B) are shown at a pitch angle of 80° for clarity.

from the system by adding 3−5 mL of Tris buffer at a flow rate of 0.05 mL/min. Vesicles were deposited by infusion of the SUV solution into the fluid cell to form a copopulation of adsorbed protein molecules and lipid vesicles on the mica surface. The density of the vesicular layer was controlled by manipulating dilution of SUVs and the incubation time in the fluid cell and monitoring by AFM imaging. Vesicles were adsorbed from solutions as prepared and down to 8× dilution, and for time periods of 1−2 h. Bilayers formed from vesicles at 8× dilution were found to be discontinuous. Infusion of a Ca^{2+}-containing Tris buffer into the system initiated vesicle fusion and reconstitution of the adsorbed platelet integrin molecules in a lipid bilayer. These events were continuously imaged by tapping mode AFM.

In Situ Incubation of Ligands with Reconstituted Integrin Receptors Adsorbed on Mica. Nanogold-conjugated peptides or fibrinogen protein ligands were incubated with the reconstituted integrins in the presence of 2 mM Mn^{2+} and at room temperature for 30−90 min. Solutions of 200−500 ng/mL fibrinogen or a 2−3 molar excess of peptide ligands were added to the cell. The fluid cell was flushed with a ∼5× excess of clean buffer to remove unbound ligands. Tapping mode AFM was used to obtain images of the functionally active reconstituted receptors bound to the ligands.

Control Experiments To Confirm Specificity of Ligand Binding. To verify that the binding of nanogold-labeled peptide ligands to reconstituted $\alpha_{IIb}\beta_3$ was specific, integrins in the supported bilayer system were blocked by RGD peptides lacking the nanogold label. This was followed by incubation with nanogold-labeled RGD peptides as described above and imaging by tapping mode AFM under buffer.

Results

AFM Imaging of $\alpha_{IIb}\beta_3$ Aggregates Bound to Ligands. Solutions of integrin $\alpha_{IIb}\beta_3$ incubated with nanogold-labeled RGD peptides as well as fibrinogen ligands were imaged by AFM in the absence of detergent. It is well-known that integrins tend to aggregate in the absence of detergent due to interactions between the transmembrane domains, and the receptors will be arranged with tails pointed inward and headgroups out.[3] We have previously shown that these aggregates could be imaged at high resolution on hydrophobic HOPG substrates.[4] Integrin/peptide ligand complexes are illustrated in Figure 1 and show that $\alpha_{IIb}\beta_3$ aggregates appeared as rosettes with headgroups pointed outward (Figure 1A). Nanogold-labeled RGD peptide ligands were visible in phase images, and appeared to be bound to the globular headgroups at the periphery of the rosette, consistent with a head out arrangement (Figure 1B). Magnified images (Figure 1C,D) of one aggregate show each individual receptor in the rosette and the corresponding nanogold-coupled peptide ligand in the phase image of the same area.

Fibrinogen ligands were observed as extensions from integrin aggregates, as shown in Figure 2. Because fibrinogen was present at a 5:1 molar ratio with the integrin, a number of nonspecifically adsorbed fibrinogen molecules were seen in the images. Fibrinogen was observed as extensions from integrin aggregates in the height images (Figure 2), but phase images did not reveal any additional information (images not shown). Integrin aggregates are not seen as clearly in these images as they were in the peptide ligand experiments shown in Figure 1. We believe that the fibrinogen molecules occasionally cross-link integrins within the aggregates, thereby hiding the headgroups and forming a nondescript mass. Cross-

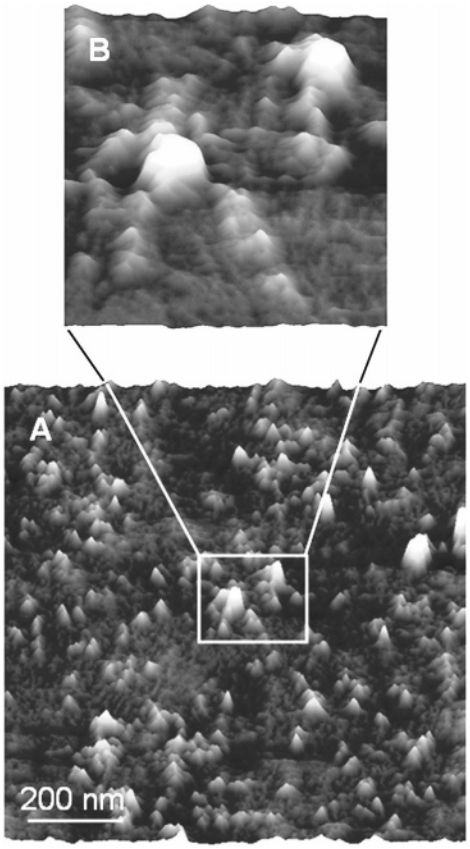

Figure 2. AFM images of fibrinogen ligands bound to integrin in detergent-free buffer and adsorbed to an HOPG substrate. (A) Topography images showing a mixture of integrin aggregates with fibrinogen molecules extending outward and nonspecifically adsorbed fibrinogen molecules. (B) Higher magnification image of the highlighted area showing more clearly the aggregates and fibrinogen extensions. The *Z* scale is 3 nm, and the pitch angle is 80°.

sectional analysis of the extensions from the integrin aggregates (data not shown) showed features consistent with the structure of fibrinogen, although the trinodular structure was not as clearly observed as it has been in single-molecule studies.[28,29]

AFM Imaging of Integrins in Supported Lipid Membranes. As described in the previous section, incubation and imaging in the absence of detergent result in aggregates of the receptor−ligand complexes. To observe single receptor−ligand binding, an in situ model system of reconstituted $\alpha_{IIb}\beta_3$ molecules in a supported lipid bilayer was prepared, as illustrated in Figure 3. A freshly cleaved mica surface yielded a clean background prior to infusion of integrin receptors and lipid vesicles into the AFM fluid cell (Figure 3A). Adsorption of integrin molecules and vesicles was seen as mixed, nondescript bumps forming a copopulation on the mica surface when imaged in Ca^{2+}-free buffer (Figure 3B). Integrin $\alpha_{IIb}\beta_3$ reconstitution was initiated by addition of Ca^{2+}, resulting in fusion of vesicles to form a bilayer containing individual integrin receptors. The transition to a lipid bilayer is seen in Figure 3C, while the fully formed bilayer containing the reconstituted integrin is shown in Figure 3D. This model system of reconstituted $\alpha_{IIb}\beta_3$ in a lipid bilayer performed in the AFM fluid cell assembly served as the substrate for the investigation of $\alpha_{IIb}\beta_3$ receptor−ligand binding.

(28) Marchant, R. E.; Barb, M. D.; Shainoff, J. R.; Eppell, S. J.; Wilson, D. L.; Siedlecki, C. A. *Thromb. Haemostasis* **1997**, *77*, 1048.
(29) Agnihotri, A.; Siedlecki, C. A. *Langmuir* **2004**, *20*, 8846.

Figure 4 shows a bearing analysis from the images of the copopulation of vesicles and integrins (as shown in Figure 3B) and after fusion of vesicles to form a bilayer containing integrins (as shown in Figure 3D). Prior to fusion, the distribution of the height is broad (Figure 4A) as it is composed of the substrate height (the mica surface) and a wide distribution of bumps corresponding to both lipid vesicles and integrins. After fusion, the distribution narrows significantly as it arises from the heights of the integrins and the lipid bilayer only. The narrow distribution suggests that most of the integrins are oriented in the same direction, headgroup up, although a small number may be improperly oriented.

AFM Images of RGD-Containing Peptide Binding to $\alpha_{IIb}\beta_3$ Receptors. Figure 5 shows images of reconstituted $\alpha_{IIb}\beta_3$ in the lipid bilayer before and after incubation with the nanogold-labeled peptide. In the absence of nanogold label, integrins were observed in the height image (Figure 5A) but no features were seen in the phase image (Figure 5B). Following addition of the RGD peptide, there were no obvious changes in the height images (Figure 5C) but marked differences in the phase images showing the mechanical property distribution (dark spots in Figure 5D).

Solid circles in Figure 5C illustrate a sampling of integrins in the height image that correlate with gold bead labels in the phase image (Figure 5D). Dashed circles illustrate integrin molecules visible in the height image that do not have associated gold labels, suggesting that these integrins are not functional or are not oriented properly (e.g., headgroup down). It is also possible that a small amount of unconjugated peptide was present in the system, and the imaging is unable to detect peptide that has been bound but does not have a gold label. It should be noted that the fraction of integrins that did not show a gold label was less than 10%. However, no matter what circumstance led to these few unlabeled integrins, the images demonstrate that the contrast in the phase data is a direct result of the gold bead label and indicative of ligand binding rather than simply an artifact due to the presence of the integrin receptor.

To demonstrate that ligand binding was specific to these functional receptors, unlabeled RGD peptides were incubated with the reconstituted integrins and imaged prior to (Figure 6A,B) and after (Figure 6C,D) addition of nanogold-labeled RGD peptide. Note the lack of gold beads in the second phase image (Figure 6D) after first blocking with unlabeled RGD, demonstrating specificity of binding.

AFM Imaging of Fibrinogen Ligand Binding to $\alpha_{IIb}\beta_3$ Receptors. Fibrinogen was infused into the reconstituted integrin model system, and observed bound to integrin receptors. Figure 7 shows that fibrinogen was visible in the topographic images (Figure 7A) although difficult to differentiate from the integrin. Fibrinogen was also visible in the corresponding phase image (Figure 7B). Interestingly, when fibrinogen molecules and integrin molecules were imaged on the supported lipid bilayer alone, phase images did not show differences in the mechanical properties from those of the supporting bilayer (data not shown). However, the phase images clearly show that the complex is easily visualized, and illustrate the trinodular fibrinogen structure more clearly than in the height image.

Higher magnification images of the fibrinogen/integrin complexes show clearly visible trinodular structures extending from the receptors (Figure 8). In most cases, a single fibrinogen molecule was seen extending from the integrin (Figure 8A), and $\alpha_{IIb}\beta_3$ was almost exclusively associated with the end of the fibrinogen molecule,

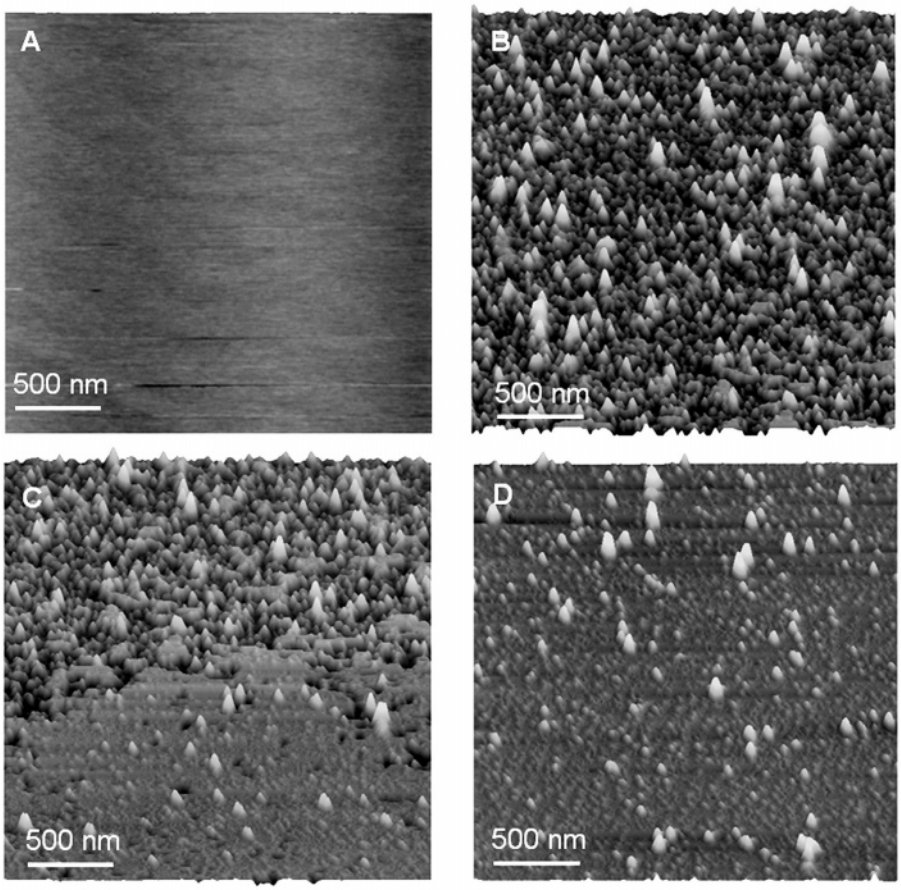

Figure 3. AFM images showing reconstitution of integrin receptors in a lipid bilayer. (A) AFM topographic image of the clean mica substrate. (B) A copopulation of vesicles and integrin. The two species are indistinguishable. (C) Images taken immediately after addition of calcium showing fusion of the bilayer. Because of the time needed to acquire an image (~8 min), it is unclear whether the image shows the bilayer advancing across the substrate or whether there was a delay and then rapid fusion during image acquisition. (D) Image taken after fusion was complete. The bumps protruding up from the bilayer are believed to be primarily integrin headgroups, although analysis of integrin binding suggests that a small number of the integrins may be oriented headgroup down. The *Z* scale is 3 nm, and the pitch angle is 80°.

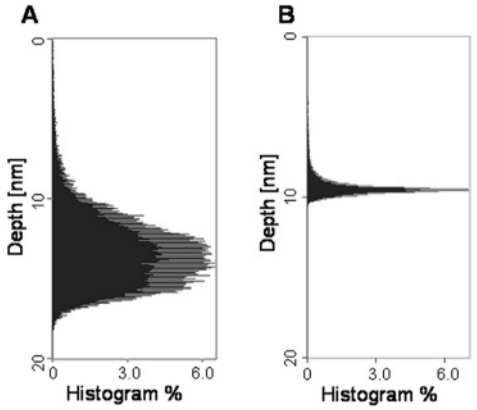

Figure 4. AFM depth analysis of (A) copopulation of integrins and vesicles and (B) reconstituted integrins in the fused bilayer. The broad and nondescript mixture becomes tightly distributed, suggesting that the majority of the integrins are likely oriented in the same direction. Functional analysis presented in subsequent sections suggests that this orientation is with headgroups protruding upward from the bilayer, although a small number of integrins may be misoriented and nonfunctional.

corresponding to the D domain of fibrinogen and the site of the γ-chain dodecapeptide. Line sketches derived from cross-sectional analysis illustrate the arrangement of the complexes (Figure 8B). Fibrinogen was also seen bridging integrin molecules (Figure 8C). Again, line sketches of the complex (Figure 8D) show that fibrinogen is bound to integrin at the D domains, similar to that observed for fibrinogen bound to single integrins. It also appears that when fibrinogen bridged integrins, receptors were located on opposite sides of the protein, consistent with the known 2-fold axis of symmetry in fibrinogen.

Discussion

Integrin-reconstituted proteoliposomes form lipid planar bilayers by fusion to quartz surfaces,[30] and the process of such bilayer formation has been demonstrated using total internal reflection fluorescence microscopy (TIR-FM).[15] In this study, we have used a reconstitution strategy for membrane proteins that bypasses the incorporation of the integrin receptor into the vesicle before fusion to the solid surface. Binding of fibrinogen ligand and nanogold-labeled RGD peptide ligands was monitored by AFM, and the data demonstrated that the integrin remained functional during the reconstitution process. Furthermore, these results demonstrate that direct imaging of individual ligand−receptor binding events can be done in a physiologically relevant in situ environment.

Imaging of integrin $\alpha_{IIb}\beta_3$ rosettes bound to ligands in the absence of detergent on hydrophobic graphite surfaces and imaging of ligand binding to individual $\alpha_{IIb}\beta_3$ molecules reconstituted in a supported lipid bilayer were

(30) Brian, A. A.; McConnell, H. M. *Proc. Natl. Acad. Sci. U.S.A.* **1984**, *81*, 6159.

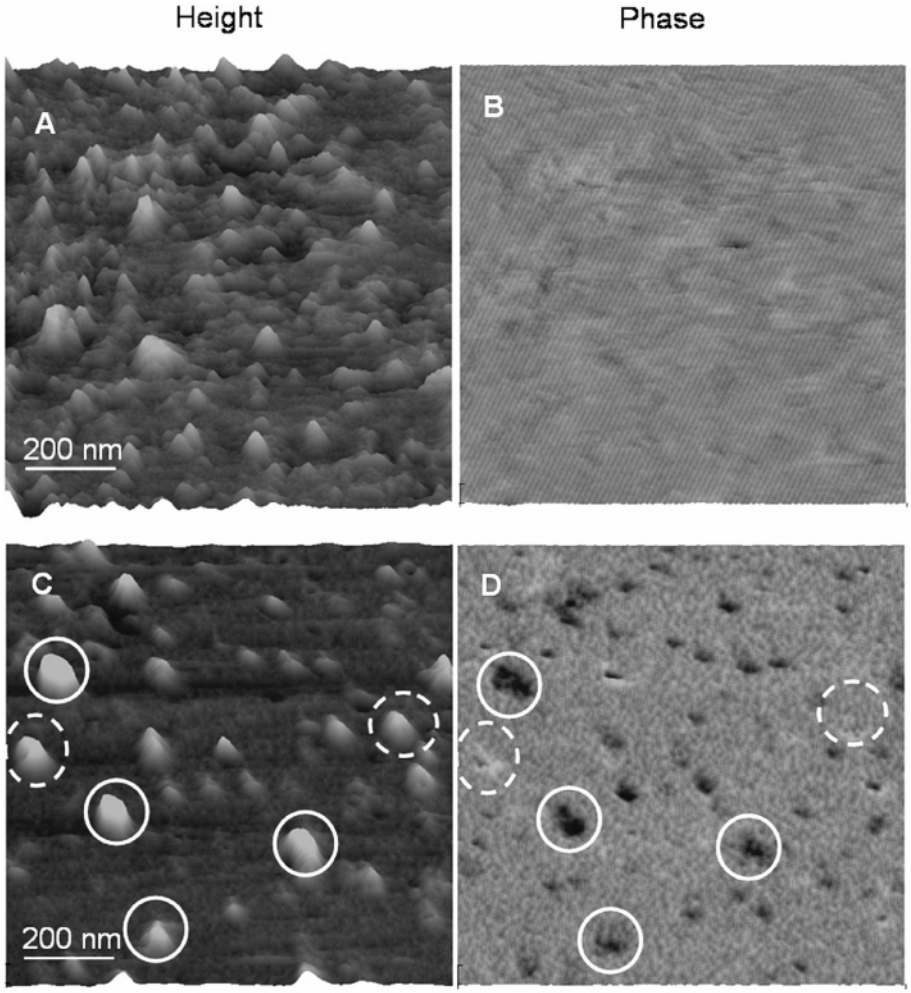

Figure 5. AFM images of gold-bead-labeled RGD peptide ligands bound to reconstituted integrins. (A) Integrins are clearly visible in the topography image prior to peptide labeling. (B) A phase image of the same area shows a uniform background, and the presence of integrins is not observable in these data. (C) the topography image (not the same area as in (A)) after addition of gold-bead-labeled peptide ligand shows no differences compared to the integrin prior to labeling. A subset of integrins is indicated by circles (both solid and dashed). (D) The phase image shows that the integrins correlate with the position of the gold bead labels, suggesting that the labeled peptides have bound to the integrin. The same subset of integrin receptors is identified in the phase image; most of the receptors have bound a ligand (solid circles), although a few do not show the gold bead label (dashed circles), suggesting they either have not bound the ligand or the ligand was not labeled. The *Z* scale is 3 nm, and the pitch angle is 80°.

performed. Images were obtained using AFM tapping mode height and phase imaging, which simultaneously measures the topography as well as the distribution of mechanical properties. Fibrinogen ligand/$\alpha_{IIb}\beta_3$ receptor complexes imaged on HOPG substrates (Figure 2) and fibrinogen ligand bound to the individual reconstituted $\alpha_{IIb}\beta_3$ molecules (Figure 8) could be seen clearly in topography images; however, peptide ligands could not be located in the height images. Therefore, nanogold-labeled peptides were used for imaging the peptide ligand/receptor complexes, and these labels were easily detected by AFM phase imaging due to differences in mechanical properties between the gold bead and the biological samples.

Nanogold reagents[31] have unique advantages because they are small and of uniform size. Lin et al.[32] demonstrated mapping of colloidal gold particles to image heparin binding sites on single fibronectin molecules by atomic force microscopy. In that study, the heparin binding site was located by measuring the location of larger 3.5−6.5 nm diameter gold particles coated with heparin and incubated with the fibronectin. In this current study, high-resolution tapping mode phase imaging has enabled us to directly visualize peptide binding on $\alpha_{IIb}\beta_3$ molecules in rosettes formed in the absence of detergent (Figure 1) as well as both individual $\alpha_{IIb}\beta_3$ molecules and integrin aggregates reconstituted into a lipid bilayer (Figure 5) by detecting the presence of the nanogold label at the headgroup of the receptor. This phase contrast imaging associated with the tapping mode adds new capabilities to the study of molecular interactions by utilizing mechanical properties for contrast of these small nanogold-labeled ligands that are otherwise difficult to resolve in height images.

AFM phase imaging has been utilized extensively to map differences in surface properties including adhesion and viscoelasticity.[33−36] The dark spots in the phase image (Figure 5D) qualitatively show the presence of nanogold-labeled peptide ligands bound to the reconstituted $\alpha_{IIb}\beta_3$

(31) Hainfeld, J. F.; Powell, R. D. *Cell Vision* **1997**, *4*, 408.
(32) Lin, H.; Lal, R.; Clegg, D. O. *Biochemistry* **2000**, *39*, 3192.
(33) Pang, G. K.; Baba-Kishi, K. Z.; Patel, A. *Ultramicroscopy* **2000**, *81*, 35.
(34) Nagao, E.; Dvorak, J. A. *Biophys. J.* **1999**, *76*, 3289.
(35) Holland, N. B.; Marchant, R. E. *J. Biomed. Mater. Res.* **2000**, *51*, 307.
(36) Garrett, J. T.; Siedlecki, C. A.; Runt, J. *Macromolecules* **2001**, *34*, 7066.

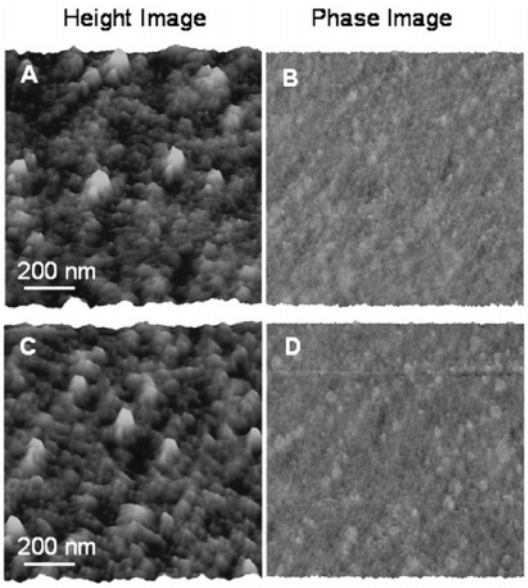

Figure 6. AFM images showing control experiments to verify specificity of binding. (A) Topography image showing integrins following incubation of unlabeled RGD peptide. (B) Phase image showing no effect of RGD labeling. (C) Topography image (not the same area as in (A)) after incubation of the RGD-blocked integrin with gold-bead-labeled RGD peptide. Again no differences can be seen in the topography of the integrins. (D) Phase image after incubation of the RGD-blocked integrin with gold-bead-labeled RGD peptide. There is no evidence of gold beads in the phase image, demonstrating successful blocking of the integrin by the unlabeled peptide. The *Z* scale is 3 nm, and the pitch angle is 80°.

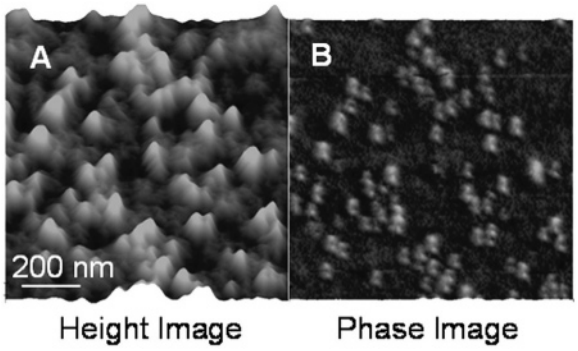

Figure 7. AFM images of reconstituted integrins after incubation with fibrinogen ligand. (A) Topographic images show there are a number of additional features compared to images of pure integrin, although fibrinogen is not clearly identified at this magnification. (B) Phase images show structures not visible prior to addition of fibrinogen. Small molecules consistent with the shape of fibrinogen are visible, and were used to direct higher magnification imaging of the complexes. The *Z* scale is 3 nm, and the pitch angle is 80°.

molecules. This phase-contrast image clearly shows a difference against the control, with well-defined spots corresponding to receptors in the height image, although the ligands are not visible in the topography. At the same time, the lack of these spots relative to a small number of integrin molecules in the height image (dashed circles in Figure 5C,D) reflects that some receptors are not bound to nanogold-coupled ligands, and are clearly different in the phase image, demonstrating that this contrast does not arise from artifacts of the protein imaging.

Fibrinogen imaged following nonspecific adsorption to a lipid bilayer lacking integrins showed "smearing" in the phase image (data not shown), suggesting that the proteins were not attached firmly enough to withstand the AFM

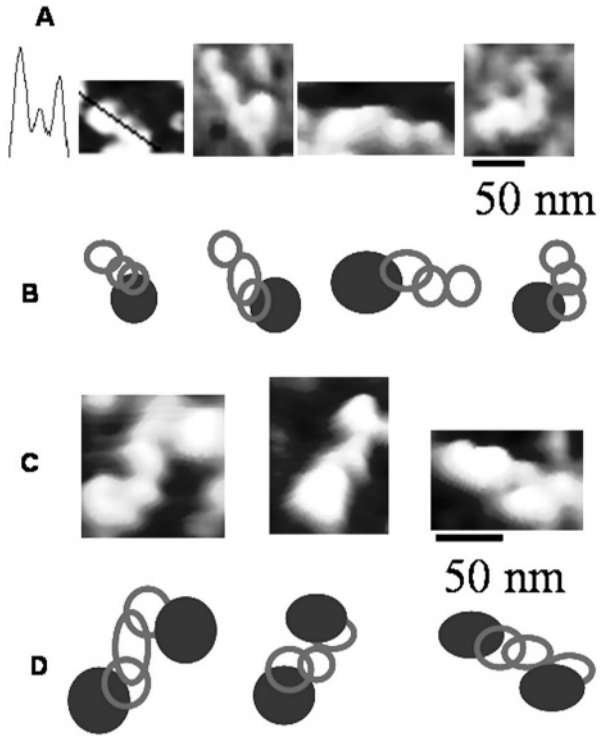

Figure 8. High-magnification AFM images of fibrinogen bound to integrin receptors. (A) An array of topography images showing trinodular fibrinogen molecules extending from the receptors. A cross-section shows the trinodular structure of an individual fibrinogen molecule. (B) Sketches of the images derived from cross-sectional analysis show that binding always occurs through the D domain of fibrinogen, and generally on the side of the molecule, consistent with the location of the γ-chain dodecapeptide. Integrins in the line sketch are shown filled; fibrinogen is shown open. (C) Occasionally, fibrinogen molecules were observed bridging integrin molecules. (D) Line sketches of these complexes again show the fibrinogen to interact through the D domain, and show that each integrin binds to one side of the fibrinogen molecule, consistent with the 2-fold axis of symmetry found in fibrinogen.

imaging force. Similarly, integrin receptors reconstituted into the lipid bilayer were not apparent in the phase images as demonstrated in Figure 5B. This lack of phase contrast may be due to insufficient mechanical stability of the receptor molecules in the egg PC lipid bilayer that is in the fluid phase at room temperature. This is a somewhat surprising result given how clearly the integrins could be seen in the topography images. However, fibrinogen bound to the reconstituted $\alpha_{IIb}\beta_3$ molecules was clearly observed in both topography and phase images (Figure 7). We believe that the binding of the (roughly horizontally oriented) fibrinogen to the (roughly vertically) reconstituted $\alpha_{IIb}\beta_3$ offers two-dimensional stabilization to the receptor−ligand complex, through both the transmembrane region of the receptor and the lateral face of fibrinogen, thereby generating sufficient mechanical stability to be observed in the phase contrast images.

Integrin $\alpha_{IIb}\beta_3$ can be activated in platelets by either inside-out signaling or outside-in signaling.[37−39] Outside-in signaling arises from binding of ligands to the $\alpha_{IIb}\beta_3$ integrin receptors and leads to platelet activation. A small percentage of isolated and purified $\alpha_{IIb}\beta_3$ molecules, up to

(37) Takagi, J.; Petre, B. M.; Walz, T.; Springer, T. A. *Cell* **2002**, *110*, 599.
(38) Shimaoka, M.; Takagi, J.; Springer, T. A. *Annu. Rev. Biophys. Biomol. Struct.* **2002**, *31*, 485.
(39) Shimaoka, M.; Springer, T. A. *Nat. Rev. Drug Discovery* **2003**, *2*, 703.

5−10%, have been shown to acquire similar activity.[3,40] In this study, the isolated $\alpha_{IIb}\beta_3$ integrins were incubated with fibrinogen ligands in the presence of Mn^{2+}, reported to activate integrin molecules,[37,38] and we observed the majority of $\alpha_{IIb}\beta_3$ molecules bound a ligand (Figures 5 and 6). Bovine serum albumin and other nonspecific blocking agents were not used in this study as they would appear in AFM images and interfere with imaging of receptors and ligands. However, nonspecific adsorption does not appear to be a problem, given the lack of fibrinogen-like structures observed in the background of the images.

Lipid bilayers may be considered as mimics of the platelet membrane, and the use of such mimetic experimental conditions has considerable advantages for visualizing dynamic processes as opposed to dry techniques.[3] However, there still remains uncertainty over whether these models adequately represent the interaction of ligands with $\alpha_{IIb}\beta_3$ on platelets. The literature shows that isolated $\alpha_{IIb}\beta_3$ molecules bind to fibrinogen and that this binding could be inhibited using peptides or antibodies in vitro, similar to that seen with intact platelets.[40,41] In this in vitro model, a large percentage of $\alpha_{IIb}\beta_3$ molecules are reconstituted as functional receptors with tails buried into the lipid bilayer and with headgroups facing up from the bilayer and available for binding. This ligand binding was inhibited by RGD peptide incubation as seen in Figure 6. Fibrinogen molecules contact the reconstituted $\alpha_{IIb}\beta_3$ headgroup at the D domain (located at the two ends of fibrinogen), consistent with the location of the integrin binding γ-chain dodecapeptide. Similarly, fibrinogen molecules that bridged the integrins showed the receptors were bound on opposite sides of fibrinogen, as expected given the 2-fold axis of symmetry in the protein. These observations are consistent with images of receptor−ligand complexes observed by electron microscopy,[3] and demonstrate that this model system yields functionally active integrins useful for in vitro measurements of platelet integrin binding events.

Conclusions

High-resolution AFM was used to perform functional imaging of complexes of integrin receptor $\alpha_{IIb}\beta_3$ with both fibrinogen and peptide (RGD heptamer labeled with 1.4 nm nanogold) ligands formed in solution as well as in a model in vitro system. In the absence of detergent, integrins aggregated with headgroups pointing outward. Fibrinogen ligands were visible as extensions from the aggregates; peptide ligands were not visible in the topographic image, but gold labels attached to the peptides were clearly observed in the phase images. Reconstituting the integrins in a model lipid bilayer yielded a large number of individual receptors arranged with the headgroup up and available for binding. Binding of both peptide and protein ligands to these receptors was observed, indicating that the receptors could retain functional activity during reconstitution. Blocking with RGD peptide inhibited ligand binding, demonstrating that interactions occurred due to specific recognition between the ligands and receptors. Fibrinogen binding to the ligands appeared to add mechanical stability to the receptors and allowed the complex to be visualized in phase images, presumably through a combination of lateral and vertical interactions of the complex with the bilayer. Analysis of individual fibrinogen/receptor interactions showed that fibrinogen preferentially bound to the integrin on the side of the outer D domains, consistent with the location of the fibrinogen γ-chain. Occasionally, fibrinogen molecules were observed bridging integrins, and in these situations the receptors were observed to again bind at the D domain of fibrinogen but on opposite sides of the protein, consistent with the 2-fold axis of symmetry in the molecule. These studies demonstrate that in vitro visualization of receptor/ligand complexes down to the level of a single binding event can be achieved by high-resolution imaging, and offer new opportunities for studying individual protein interactions in situ and under physiologic conditions.

Acknowledgment. We acknowledge financial support from the American Heart Association and the Whitaker Foundation through The Biomedical Engineering Institute at The Pennsylvania State University College of Medicine. We are thankful to Dr. Henry Donahue in the Musculoskeletal Research Laboratory and the Center for Biomedical Devices and Functional Tissue Engineering, as well as Dr. Tao Lowe in the Biomedical Engineering Institute for access to equipment. We also acknowledge Dr. Keith Milner for valuable technical assistance and discussions.

LA046943H

(40) Steiner, B.; Cousot, D.; Trzeciak, A.; Gillessen, D.; Hadvary, P. *J. Biol. Chem.* **1989**, *264*, 13102.
(41) Parise, L. V.; Phillips, D. R. *J. Biol. Chem.* **1985**, *260*, 10698.